ESTIMATING EMISSIONS OF 20 VOCs. I: SURFACE AERATION

By Chu-Chin Hsieh,[1] Kyoung S. Ro,[2] and Michael K. Stenstrom,[3] Member, ASCE

ABSTRACT: The emission rates of semivolatile organic compounds during surface aeration can be estimated from the oxygen mass-transfer coefficient $K_L a_{O_2}$ and a modified coefficient Ψ_M, which incorporates the fraction of liquid-phase mass-transfer resistance to total resistance. In order to verify this method, the mass-transfer coefficients for oxygen and 20 volatile organic compounds (VOCs) were simultaneously measured in a laboratory-scale surface-aerated reactor. Using these measurements, the ratios of gas-phase and liquid-phase mass-transfer coefficients were determined by nonlinear regression. These ratios then were used to estimate the fraction of liquid-phase resistance to total resistance. The method was validated by excellent agreement between observation and theory. The correlation between the ratios of gas- and liquid-phase transfer coefficients and specific power input was also studied.

INTRODUCTION

The 1990 Clean Air Act Amendments identified volatile organic compounds (VOC) emissions from publicly owned treatment works (POTWs) as a major source category. Indirect estimation of VOC emissions from the aeration basin using oxygen as a surrogate is a valuable and cost-effective approach for engineering applications. Based upon the proportionality of mass-transfer coefficients, previous researchers (Smith et al. 1980; Matter-Mueller et al. 1981; Roberts et al. 1983, 1984) have defined the ratio of mass-transfer coefficients for a VOC to oxygen as Ψ. This ratio, along with the oxygen-transfer coefficient $K_L a_{O_2}$, is now widely used to estimate VOC emissions from quiescent and aerated water surfaces. The approach is popular because of its ease of use and the availability of oxygen-transfer information.

The development of the Ψ concept is based upon the two-resistance mass-transfer model and the assumption that gas-phase resistance is negligible. Neglecting gas-phase resistance restricts the concept's use to highly volatile compounds such as oxygen, carbon tetrachloride, and 1,1,1-trichloroethane. The concept, if applied to semivolatile compounds, overestimates the mass-transfer rate because gas-phase resistance is no longer negligible. The object of this research project was to develop an improved method that includes the impact of gas-phase resistance and can be used to estimate transfer rates of compounds with a wide range of volatilities or Henry's coefficients. This is the first paper in a three-part series, and reports the theoretical development of Ψ_M and results for surface-aeration systems. (Subsequent papers

[1]Sr. Engr., Montgomery Watson, Inc., P.O. Box 7009, Pasadena, CA 91109-7009.
[2]Asst. Prof., Civ. Engrg. Dept., Louisiana State Univ., Baton Rouge, LA 70803-6405.
[3]Prof., Civ. Engrg. Dept., 4173 Engrg. I, Univ. of California, Los Angeles, CA 90024-1600.

Note. Discussion open until May 1, 1994. Separate discussions should be submitted for the individual papers in this symposium. To extend the closing date one month, a written request must be filed with the ASCE Manager of Journals. The manuscript for this paper was submitted for review and possible publication on May 15, 1992. This paper is part of the ***Journal of Environmental Engineering***, Vol. 119, No. 6, November/December, 1993. ©ASCE, ISSN 0733-9372/93/0006-1077/$1.00 + $.15 per page. Paper No. 4059.

will report on diffused aeration, turbine aeration, the impact of surfactants, and scale-up.)

BACKGROUND

Henry's Coefficient

Henry's law describes the equilibrium between air and water phases at dilute concentration, as follows:

$$H_c = \frac{C_G^*}{C_L} \quad \ldots\ldots (1)$$

where H_c = dimensionless Henry's coefficient; C_G^* = gas-phase concentration in equilibrium with the liquid-phase concentration, C_L (expressed in same units). Henry's coefficients can also be estimated from the pure solute vapor pressure and its solubility, as follows:

$$H = \frac{PM}{S} \quad \ldots\ldots (2)$$

where H = Henry's coefficient [(atm m^3/mol)]; P = vapor pressure of the pure solute (atm); M = gram molecular weight of the solute (g/mol); and S = solubility of the solute in water (g/m^3).

The larger the Henry's coefficient, the greater the equilibrium concentration of solute in air and the more easily it is stripped during aeration. It is difficult to experimentally determine Henry's coefficients, and there are large differences between published values by various investigators. Mackay and Shiu (1981) reviewed Henry's coefficients for environmentally relevant chemicals and found that considerable discrepancies exist in the literature, even for common chemicals. The coefficients used in this study were determined experimentally, and are listed in Table 1. Several vary from published values.

Relationship of Mass-Transfer Coefficient to Diffusivity

The major resistance to mass transfer at the gas-liquid interface is the diffusional resistance in each phase. Various models have been proposed to describe mass transfer to the phase boundary. The best known models are based on Fick's law, and predict that the mass-transfer coefficient k is proportional to some power of the molecular diffusivity, D

$$k \propto D^n \quad \ldots\ldots (3)$$

where k = mass-transfer coefficient; D = molecular-diffusion coefficient; and n = 1.0 for the two-film theory (Lewis and Whitman 1924); and 0.5 for the penetration theory (Higbie 1935) and surface-renewal theory (Danckwerts 1951).

Postulating that the film and surface-renewal equations are limiting cases of a more-general equation, Dobbins (1956) proposed a combined film-surface renewal theory, with n varying from 0.5 to 1.0 depending on the turbulence in the system. Under sufficiently turbulent conditions, n approaches 0.5 (surface renewal or penetration theory); under laminar, or less turbulent, conditions n approaches 1.0 (film theory).

The resistance to mass transfer across an interface is the sum of the resistances in each phase. This concept was proposed by Lewis and Whitman in 1924 as the two-film theory; as Treybal (1968) pointed out, their two-

TABLE 1. Properties of 20 VOCs Studied (at 760 mmHg; 20°C)

Compound (1)	Formula (2)	Abbreviation (3)	Molecular weight (g/mole) (4)	H_c (5)	$D_L \times 10^6$ (cm^2/s) (6)	$D_G \times 10^2$ (cm^2/s) (7)	Retention time (min) (8)
Oxygen	O_2	O_2	32.0	30.2	2.11	21.32	—
Benzene	C_6H_6	BZ	78.1	0.230	0.96	8.95	6.2
Bromobenzene	C_6H_5Br	BBZ	157.0	0.100	0.83	7.28	17.7
Bromoform	$CHBr_3$	BF	252.8	0.041	0.93	7.65	16.4
Carbon tetrachloride	CCl_4	CT	153.8	1.316	0.92	8.16	5.8
Chlorobenzene	C_6H_5-Cl	CBZ	112.6	0.150	0.86	7.75	14.1
Chloroform	$CHCl_3$	CLF	119.4	0.160	1.01	8.93	5.2
1,2-Dichlorobenzene	$C_6H_4Cl_2$	12DCB	147.0	0.087	0.78	6.91	21.8
1,3-Dichlorobenzene	$C_6H_4Cl_2$	13DCB	147.0	0.120	0.78	6.94	20.5
1,4-Dichlorobenzene	$C_6H_4Cl_2$	14DCB	147.0	0.110	0.76	6.83	20.8
1,2-Dichloroethene (cis)	$CHCl{=}CHCl$	12DCE	96.9	0.170	1.05	9.45	21.8
Ethylbenzene	C_6H_5-CH_2CH_3	EBZ	106.2	0.260	0.76	7.15	14.6
Ethylenebromide	CH_2BrCH_2Br	EDB	187.9	0.041	0.97	8.11	12.8
Naphthalene	$C_{10}H_8$	NAPH	128.2	0.038	0.72	6.48	27.3
Perchlorothylene	$CCl_2{=}CCl_2$	PCE	165.8	0.570	0.89	7.77	11.9
1,1,1-Trichloroethane	CCl_3CH_3	111TCA	133.4	0.530	0.90	8.18	5.5
1,1,2,2-Tetrachloroethane	$CHCl_2CHCl_2$	1122TCA	167.9	0.042	0.82	7.21	18
Toluene	C_6H_5-CH_3	TLN	92.1	0.230	0.84	7.92	10.6
Trichloroethylene	$CCl_2{=}CHCl$	TCE	131.4	0.250	0.96	8.48	7.6
1,2-Xylene (O)	C_6H_4-$(CH_3)_2$	OXY	106.2	0.180	0.77	7.16	15.9
1,3-Xylene (m)	C_6H_4-$(CH_3)_2$	MXY	106.2	0.240	0.76	7.12	14.9

film theory does not depend on the validity of the film theory. Therefore, the "two-resistance" theory would be a more-appropriate name. In this paper we use the term two-resistance model instead of the two-film theory to denote that n can be different from 1.0. A common convention used here and in engineering applications is to combine the mass-transfer coefficients and the interfacial area into a single parameter $K_L a$.

Ψ_M Concept Development

Under the assumption of dominant liquid-phase resistance to mass transfer, the proportionality of liquid-phase mass-transfer coefficients between a VOC and oxygen is denoted as Ψ

$$\Psi = \frac{K_L a_{VOC}}{K_L a_{O_2}} = \frac{k_L a_{VOC}}{k_L a_{O_2}} = \left(\frac{D_{LVOC}}{D_{LO_2}}\right)^n \quad \ldots\ldots\ldots\ldots\ldots\ldots\ldots\ldots (4)$$

where Ψ = ratio of the mass-transfer coefficients of the VOC to oxygen (dimensionless); $k_L a_{VOC}$, $k_L a_{O_2}$ = liquid-phase mass-transfer coefficients of the VOC and oxygen ($1/t$); D_{LVOC}, D_{LO_2} = liquid diffusivities for the VOC and oxygen (L^2/t); and $K_L a_{VOC}$, $K_L a_{O_2}$ = overall mass-transfer coefficients for the VOC and oxygen ($1/t$).

The general mathematical expression for the two-resistance model is as follows:

$$\frac{1}{K_L a_{VOC}} = \frac{1}{k_L a_{VOC}} + \frac{1}{H_c k_G a_{VOC}} \quad \ldots\ldots\ldots\ldots\ldots\ldots\ldots\ldots (5)$$

where $k_G a_{VOC}$, $k_L a_{VOC}$ = gas- and liquid-phase mass-transfer coefficients of the VOC ($1/t$). The fraction of liquid-film resistance (R_L) to total resistance (R_T) can be expressed as follows:

$$\frac{R_L}{R_T} = \frac{R_L}{R_L + R_G} = \frac{1}{1 + \dfrac{R_G}{R_L}} = \frac{1}{1 + \dfrac{1}{H_c \dfrac{k_G a}{k_L a}}} \quad \ldots\ldots\ldots\ldots\ldots\ldots\ldots\ldots (6)$$

where R_L, R_T = liquid- and gas-phase resistances, respectively (dimensionless). Rearranging (5) and multiplying both sides by $1/(k_L a_{VOC})$ gives

$$\frac{K_L a_{VOC}}{k_L a_{VOC}} = \frac{1}{1 + \dfrac{1}{H_c \dfrac{k_G a}{k_L a}}} \quad \ldots\ldots\ldots\ldots\ldots\ldots\ldots\ldots\ldots\ldots\ldots\ldots (7)$$

The proportionality of overall VOC and oxygen mass-transfer coefficients can be expressed as Ψ_M

$$\Psi_M = \frac{K_L a_{VOC}}{K_L a_{O_2}} \quad \ldots\ldots\ldots\ldots\ldots\ldots\ldots\ldots\ldots\ldots\ldots\ldots\ldots\ldots\ldots\ldots (8)$$

In the case of oxygen, a highly volatile compound (H_c = 30.2 at 20°C), we see that 99% of the resistance is in the liquid phase for $k_G a/k_L a > 3$ [from (6)], therefore, $k_L a_{O_2} = K_L a_{O_2}$, and

$$\Psi_M \approx \frac{K_L a_{VOC}}{k_L a_{O_2}} \quad \ldots\ldots (9)$$

Multiplying the numerator and denominator of (9) by $k_L a_{VOC}$ gives

$$\Psi_M = \frac{k_L a_{VOC}}{k_L a_{O_2}} \frac{K_L a_{VOC}}{k_L a_{VOC}} \quad \ldots\ldots (10)$$

Substituting (4) and (7) into (10) results in

$$\Psi_M = \frac{K_L a_{VOC}}{K_L a_{O_2}} = \left(\frac{D_{LVOC}}{D_{LO_2}}\right)^n \frac{R_L}{R_T} = \Psi \frac{R_L}{R_T} \quad \ldots\ldots (11a)$$

where Ψ_M = modified Ψ-value (dimensionless); and

$$\Psi = \frac{k_L a_{VOC}}{k_L a_{O_2}} = \left(\frac{D_{LVOC}}{D_{LO_2}}\right)^n \quad \ldots\ldots (11b)$$

(dimensionless).

We can use (11*a*) to estimate emission rates for volatile and semivolatile compounds if the mass-transfer coefficient of oxygen and the fraction of liquid-film resistance are known. To conveniently estimate the volatilization rate of a particular compound (11*a*) can be rearranged as

$$K_L a_{VOC} = \frac{\Psi}{1 + \dfrac{k_L a_{VOC}}{H_c k_G a_{VOC}}} K_L a_{O_2} = \Psi_M (K_K a_{O_2}) \quad \ldots\ldots (12)$$

We see that we can calculate the fraction of liquid-film resistance from the ratio of the gas film to liquid film mass-transfer coefficients and Henry's coefficient.

Analysis of Gas- and Liquid-Phase Mass-Transfer Coefficients

Based upon the relationship of mass-transfer coefficient to diffusivity, $k_L a$ is proportional to D_L^n and $k_G a$ is proportional to D_G^m, where D_L and D_G are the molecular diffusivities in water and air, respectively.

Liquid-film side

$$k_L a_{VOC} = k_L a_{O_2} \left(\frac{D_{LVOC}}{DL_{O_2}}\right)^n \quad \ldots\ldots (13)$$

Gas-film side

$$k_G a_{VOC} = k_G a_{O_2} \left(\frac{D_{GVOC}}{DG_{O_2}}\right)^m \quad \ldots\ldots (14)$$

If we substitute (13) and (14) into the two-resistance equation [(5)], we obtain

$$\frac{1}{K_L a_{VOC}} = \frac{1}{k_L a_{O_2} \left(\dfrac{D_{LVOC}}{D_{LO_2}}\right)^n} + \frac{1}{(H_c) k_G a_{O_2} \left(\dfrac{D_{GVOC}}{DG_{O_2}}\right)^m} \quad \ldots\ldots (15)$$

The validity of (15) was confirmed by Goodgame and Sherwood (1954), who measured mass-transfer coefficients for vaporization of water into air, and the absorption of carbon dioxide, ammonia, and acetone from air into water. They assumed both exponents m and n to be equal to 0.5, and found that the observed and calculated values of K_La agreed well. Their data support the concept of adding individual phase resistances, and suggest that overall coefficients may be reliably calculated from the individual coefficients. Munz and Roberts (1984) used this approach.

Best-Fit Parameters

To use nonlinear regression to estimate parameters from experimental results, (15) was rearranged as follows:

$$X = AY^n + WBZ^m \quad (16)$$

where $X = (K_La_{VOC})^{-1}$; $Y = (D_{LVOC}/D_{LO_2})^{-1}$; $Z = (D_{GVOC}/D_{GO_2})^{-1}$; $W = 1/H_c$; $A = 1/(k_La_{O_2})$; $B = 1/(k_Ga_{O_2})$; n = exponent of liquid diffusivity; m = exponent of gas diffusivity; and $A/B = (k_Ga_{O_2})/(k_La_{O_2})$.

Eq. (16) has four knowns (X, Y, Z, and W) and four unknowns (A, B, m, and n). The exponents m and n were assumed to be equal and are referred to as mn. The reason for this assumption was discussed by Munz and Roberts (1984). Applying this assumption leaves three parameters—A, B, and mn—which need to be estimated by regression.

The nonlinear regression (NLIN) procedure with a statistical analysis system (*SAS* 1982) was used to determine A, B, and mn using the least-squares fit. After a grid of values was specified, NLIN evaluates the residual sum of squares at each combination of values to determine the best set of values to start the iterative algorithm. The algorithm uses the residuals of the partial derivatives with respect to the parameters to estimate new parameter values in an iterative fashion until no further reduction in the sum of squares is possible. The procedure was initially tested using data from Roberts and Dandliker (1983). The additional degrees of freedom (20 compounds used in this study compared to six compounds used by Roberts and Dandliker) provided greater confidence and precision in the parameter estimates.

EXPERIMENTAL METHODS

Table 1 shows the properties of the organic compounds chosen for this study. The 20 organic compounds span a wide range of volatility with liquid- and gas-phase controlled conditions. The value of Henry's coefficient (H_c) is the single most important factor for determining the transfer rate, and reported values for VOCs can differ by more than 50% (Baillod et al. 1990). Therefore, values of H_c were chosen on the basis of either agreement among various sources (Mackay and Shiu 1981; Verschueren 1977) or the best fit from our results, when our results fell within the range of literature estimates. In addition, Henry's law coefficients for selected compounds were confirmed experimentally (Hsieh 1991) using EPICS (equilibrium partitioning in closed systems) procedure (Gossett 1987).

Methanol was present in the systems, since it was used as a solvent in preparation of the stock mixtures that were introduced into the reactor. The use of solute mixtures and the presence of methanol may change Henry's coefficients and oxygen-transfer coefficient. Munz and Roberts (1986, 1987) found no effects of organic mixtures on the Henry's coefficients for PCE,

TCE, 1,1,1-TCA, chloroform, and dichloromethane in an aqueous mixture of the five compounds with a total mixture concentrations of up to 375 mg/L. Gossett (1987) verified that measurements of Henry's coefficients in dilute, aqueous mixtures of solutes agree well with values obtained for single solutes. In this study, the maximum total organic mixture concentration was between 20 and 40 mg/L, which is below the experimental conditions used by Munz and Roberts (1986). The cosolvent concentration of methanol in water (0.26 g/L) used in this study was also far below the effective concentration reported by Munz and Roberts (1987). They demonstrated that in excess of 10 g/L of cosolvent is required to reduce the solute's Henry's coefficient. They also determined that the cosolvent and VOCs mixture did not change the oxygen transfer coefficient.

All volatile compounds were obtained from Aldrich Chemical Co. (St. Louis, Mo.) and Fisher Scientific Co. (Pittsburgh, Pa.). Methanol was high-performance liquid-chromatography grade from Fisher Scientific Co. Fresh tap water with a conductivity between 450 and 500 S/cm was used for all gas-transfer experiments. The addition of sodium sulfite used in determining the oxygen-transfer coefficients increased the conductivity to about 650 to 700 S/cm (equivalent to 0.005 N KCl). Conductivity measurements were made with a YSI glass probe, model 3403, with a cell constant of 1.0 cm^{-1}.

Fig. 1 shows the cylindrical plexiglass reactor used in these experiments. The jacketed reactor was constructed of 40.0-cm-long sections of concentric 23.5-cm and 30.5-cm diameter plexiglass tubing. The reactor had a total volume of 17.4 L. The working volume of water was 16.0 L, with a water depth of 36.8 cm. Agitation was provided by axial-flow impellers. The impellers were marine-type impellers provided by Michigan Industrial Propellers (Grand Rapids, Mich.). The impellers were located on a common shaft 6.4 cm, 30.5 cm, and 40.0 cm from the bottom of the reactor. The

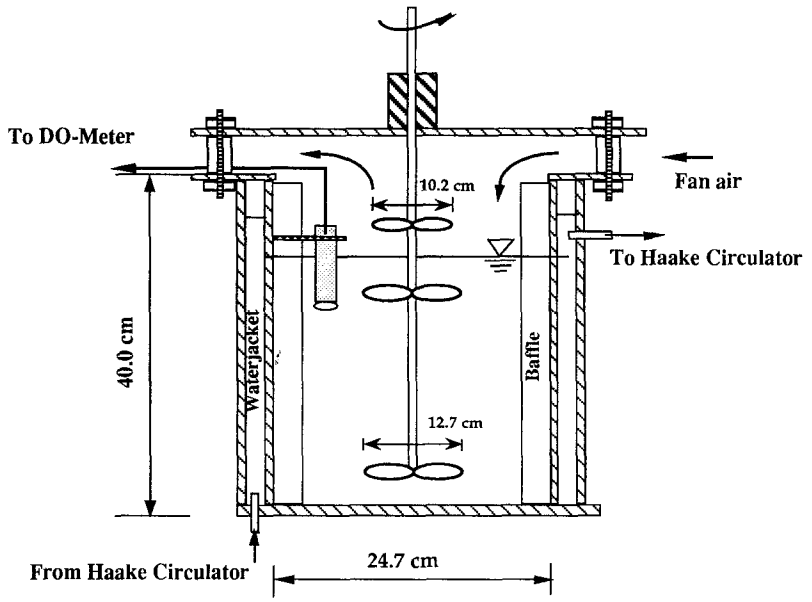

FIG. 1. Surface Aeration Reactor

upper impeller, located 3.8 cm above the water surface with a diameter of 10.2 cm and a width of 2.5 cm, served as a gas agitator to maintain complete mixing in the head space. The impellers mounted below the water surface had a diameter of 12.7 cm and a width of 3.8 cm. The middle and bottom impellers, located 7.6 and 31.7 cm below the water surface, provided liquid mixing. The reactor's cover contained a bearing to support the shaft to maintain precise impeller positions throughout the tests. The reactor had four 2.2-cm stainless-steel baffles (9.0% of the tank diameter) arranged at 90° around the circumference.

A 40.6-cm-diameter fan (Dayton, model 4C508D) was used to provide air flow across the reactor's head space. The air velocity above the water surface ranged between 1.8 and 2.4 m/s. A Haake KT 33 circulating water bath circulated water through the water jacket at a rate of up to 77.5 L/h to maintain the temperature in the reactor to within ±0.3°C of the set point (20°C). The impeller rotational speed was monitored by a General Radio Company stroboscope, type 1531-A. The Reynolds number (R), the ratio of inertia force in the impeller to viscous forces in the fluid, was used to represent the degree of turbulence in an impeller-stirred tank as follows:

$$\mathrm{R} = \frac{Da^2 N \rho}{\mu} \quad \dots\dots (17)$$

where N = rotational speed (RPM); Da = impeller diameter (m or ft); ρ = fluid density (kg/m^3 or lb/cu ft); and μ = viscosity [Pa·s or lb/(ft-s)].

Each experiment was begun by adjusting the impeller speed to the desired value using the stroboscope. After the water had been equilibrated to a constant temperature of 20°C, dissolved oxygen (DO) was removed using sodium sulfite with a cobalt chloride catalyst. The cobalt chloride dose was less than 0.5 mg/L. Theoretically, 7.9 mg/L of sodium sulfite is required for each milligram per liter of DO present. Since it is common practice to add 1.5–2.0 times of this amount to ensure complete deoxygenation, approximately 14 mg/L per mg of DO was added.

After the DO concentration was reduced to almost zero, approximately 5 mL of the VOCs dissolved in methanol was introduced with a pipette, providing approximately 1.0–2.0 mg/L initial concentrations of each VOC. After 1 min of mixing the first sample was collected and a total of 15–20 samples were taken. The sampling intervals were shorter at the beginning of a test due to the larger driving force. Samples were taken from the reactor with a 25-mL pipette and then transferred into two 9-mL hypovials and sealed with Teflon-faced rubber septa. The vials were chilled to 4°C on the day of collection and maintained at that temperature until analyzed. Samples were allowed to warm to ambient temperature before analysis. Analysis was usually completed within one day after sampling.

The oxygen concentration in the reactor was measured continuously with a DO probe (Yellow Springs Instruments, Model 58) and a standard membrane (1.0 mil) and plotted on a strip chart recorder. At the end of each test, three water samples were taken and analyzed for DO by the Winkler method (*Standard* 1985). The ASCE (1984) procedure was used to estimate oxygen-transfer coefficients.

Organic Analysis Techniques

The VOCs were analyzed by capillary gas chromatography using a purge-and-trap device and a flame-ionization detector (FID). The FID was chosen over an electron-capture detector (ECD) for its wider dynamic range. The

purge-and-trap device was a Tekmar model 00-996367-00 set with the following program: 11 min purge, 4 min desorb, and 12 min bake time. The purge-and-trap device was attached to a Hewlett-Packard model 5890 GC. Before initial use, the trap was conditioned overnight at 180°C by backflushing with an inert gas (He) flow of at least 20 mL/min. During purging, the trap was vented to the room, and not to the analytical column. Prior to beginning analysis each day, the trap was backflushed for 10 min at 180°C.

The capillary column was a J&W Scientific (Folsom, Calif.) DB-624 with a 1.8 μm film thickness and the dimensions of 30 m by 0.32 mm diameter. The gas chromatograph (GC) time and temperature program was as follows: 35°C initial temperature, 150°C final temperature, 5 min initial hold, 1 min final hold time, and a 5°C/min temperature program. The GC and purge-and-trap gas-flow rates were controlled as follows: helium carrier gas at 20.0 mL/min, hydrogen combustion gas at 47.2 mL/min, and dry-air purge gas at 314.8 mL/min. A Hewlett-Packard model 3396A integrator used to record GC output had the following settings: attenuation of 4, chart speed of 0.5 cm/min, peak width of 0.04, area rejection of 3,000, and threshold of −1. These conditions separated all 20 peaks to allow easy identification. The retention times of all compounds are shown in Table 1. Naphthalene carryover in the purge and trap was initially a problem but was reduced to 3% by heating the purge sampler at 150°C for 15 min, followed by flushing with air for 10 min between each analysis.

Liquid and Gas Diffusivities

Diffusivity was estimated as opposed to using measured literature values as suggested by Smith et al. (1980). Table 1 shows the estimated values. Liquid diffusivities were calculated with the modified Wilke-Chang estimation method [Reid et al. (1987), page 598, (11-9.1)] with parameter $\phi = 2.26$ for water. The solute molar volume at the normal boiling point, V_A, was estimated with the Tyn and Calus correlation (T&C) increments (Reid et al. 1987). The T&C increments were used because they provided molar volumes for the compounds studied between the predictions of the Le Bas additive method and the predictions of the Schroeder increments method. The Wilke and Lee correction [Reid et al. (1987), page 587, (11-4.1)] was used to estimate gas diffusivities. The solute molar volume at the normal boiling point (V_A) estimated in the liquid diffusivities was used. The Lennard-Jones potential procedure [Reid et al. (1987), page 582] was used to estimate σ_{AB} and Ω_d.

RESULTS AND COMMENT

The dependence of (P/V) on the impeller speed (N) is shown in Fig. 2. The correlation is given by

$$\frac{P}{V} = 2.05 \times 10^{-6} (N)^{3.11} \quad \ldots\ldots\ldots\ldots\ldots\ldots\ldots\ldots\ldots\ldots\ldots\ldots\ldots\ldots (18)$$

where P/V = specific power input (W/m^3); and N = rotational speed (RPM).

This correlation agrees with the (19-4) in *Perry's Chemical Engineer's Handbook* (Perry 1984) and Nagata (1975), indicating that the specific power input is proportional to the third power of the impeller speed. The power input ranged between 0.13 and 8.0 W, which is equivalent to a specific power input ranging from 8 to 500 W/m^3, which generally corresponds to

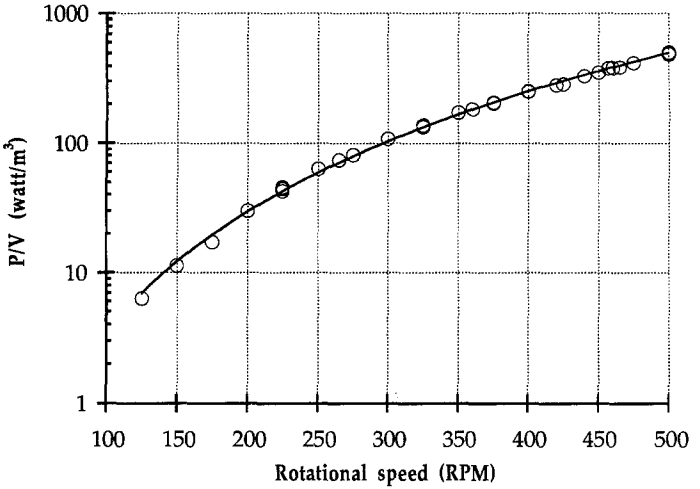

FIG. 2. Correlation between Power Input and Rotational Speed

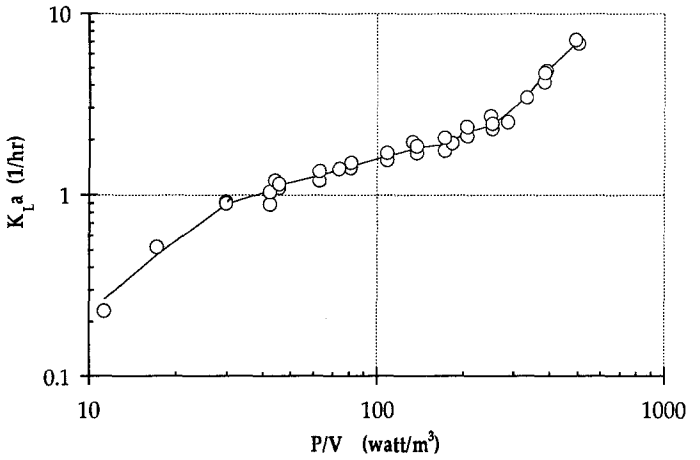

FIG. 3. Oxygen-Transfer Coefficient versus Specific Power Input

the specific power inputs found in wastewater-treatment plants (Paulson 1979; Libra 1991).

Fig. 3 shows the oxygen-transfer rate as a function of power input. The K_La-value of oxygen increased from 0.23 to 7.2 (1/h) as the impeller speed was increased from 150 to 500 RPM. Below a specific power input of 30 W/m^3, the turbulence was in the transition range. With very high power input (250 W/m^3 < P/V < 500 W/m^3), the aerator created a continuous sheet of spray and entrained air bubbles, which increased the rate of oxygen transfer dramatically. Eckenfelder et al. (1967) reported that 60% of oxygen transfer came from liquid spray and 40% from turbulence entrainment. With high air-bubble entrainment, the mass-transfer model converts from pure surface aeration to a combination of bubble and surface aeration. Currently

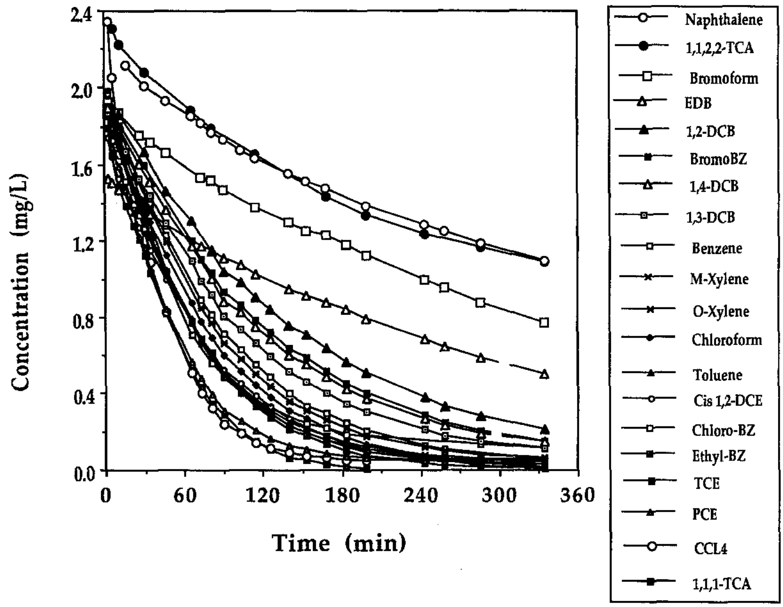

FIG. 4. Example Plot: Stripping of 20 VOCs (Impeller Speed 275 RPM)

no relationship exists to quantitatively describe this phenomenon. Therefore, this high power-density region was excluded from further analysis. For surface aeration at an unbroken water surface, Kozinski and King (1966) predicted that the mass-transfer coefficient ($K_L a$) should be proportional to $(P/V)^{0.33}$. They summarized 12 studies and reported $K_L a \approx (P/V)^n$ with, n from 0.2 to 0.4 at an unbroken air-water interface. Correlating the oxygen-transfer results from this investigation for the completely turbulent region, 30 W/m^3 < (P/V) < 250 W/m^3, with an unbroken water surface and no air-bubble entrainment, we found

$$K_L a_{O_2} = 0.17 \left(\frac{P}{V}\right)^{0.48} \quad \text{(19)}$$

The exponent found in this experiment, 0.48, is in approximate agreement with the observation reported by Kozinski and King (1966).

Fig. 4 shows an example result of the concentrations of 20 VOCs versus time during a surface-aeration experiment. In surface aeration of open vessels, sufficient air volume is provided to avoid significant gas-phase saturation above the liquid surface, which allows us to assume $C_G = 0$. Therefore, the liquid-concentration change over time was used to estimate the mass-transfer rate of each VOC as follows:

$$\ln\left(\frac{C_L}{C_{Lo}}\right) = -K_L a(t - t_o) \quad \text{(20)}$$

Using (20), the slope of a semilog plot of C_L/C_{Lo} versus $(t - t_o)$ gives us $K_L a$. Using this technique, an estimate of the initial concentration is critical

TABLE 2. Summary of Mass-Transfer Coefficients of Oxygen and 20 VOCs

VOC (1)	Test Number (1/h)													
	S20 (2)	S19 (3)	S26 (4)	S17 (5)	S22 (6)	S29 (7)	S27 (8)	S23 (9)	S28 (10)	S25 (11)	S29 (12)	S21 (13)	S24 (14)	S16 (15)
[RPM]	150	200	235	275	325	350	375	400	420	425	440	450	475	500
[P/V (w/m^3)]	11.3	30.9	50.2	80.7	133.7	167.3	206.0	250.4	290.1	300.7	331.6	353.9	420.3	491.5
O_2	0.22	0.92	1.20	1.40	1.80	1.85	2.10	2.30	2.40	2.50	2.75	3.08	4.37	7.17
CT	0.17	0.64	0.78	0.94	1.20	1.28	1.41	1.54	1.63	1.67	1.81	1.87	2.02	2.35
PCE	0.12	0.56	0.75	0.83	1.03	1.13	1.21	1.31	1.37	1.45	1.52	1.57	1.72	1.90
111TCA	0.11	0.58	0.67	0.87	1.01	1.11	1.25	1.33	1.38	1.44	1.55	1.64	1.81	2.00
TCE	0.14	0.63	0.81	0.91	1.13	1.19	1.28	1.39	1.45	1.51	1.59	1.74	1.80	1.88
EBZ	0.13	0.58	0.75	0.83	1.00	1.07	1.16	1.29	1.36	1.41	1.49	1.58	1.66	1.74
12DCE	0.14	0.63	0.83	0.95	1.18	1.23	1.30	1.41	1.46	1.49	1.58	1.65	1.75	1.89
MXY	0.14	0.57	0.65	0.85	1.05	1.10	1.19	1.28	1.35	1.41	1.47	1.59	1.71	1.74
OXY	0.13	0.57	0.71	0.82	1.05	1.12	1.20	1.28	1.33	1.42	1.44	1.63	1.71	1.74
TLN	0.14	0.60	0.77	0.87	1.08	1.19	1.26	1.33	1.37	1.46	1.51	1.60	1.86	1.95
BZ	0.13	0.61	0.75	0.86	1.05	1.17	1.26	1.33	1.34	1.46	1.51	1.60	1.86	1.95
CLF	0.12	0.55	0.71	0.81	0.99	1.05	1.13	1.25	1.29	1.36	1.42	1.49	1.58	1.62
CBZ	0.13	0.59	0.76	0.86	1.05	1.17	1.25	1.30	1.36	1.42	1.47	1.58	1.67	1.74
132DCB	0.12	0.54	0.71	0.80	1.00	1.06	1.16	1.21	1.23	1.31	1.33	1.38	1.47	1.55
12DCB	0.12	0.53	0.69	0.78	0.94	1.03	1.09	1.15	1.18	1.26	1.27	1.34	1.40	1.46
14DCB	0.13	0.55	0.72	0.81	0.98	1.08	1.15	1.21	1.23	1.31	1.33	1.39	1.47	1.53
BBZ	0.13	0.58	0.73	0.82	1.01	1.12	1.17	1.24	1.27	1.34	1.39	1.46	1.53	1.60
BF	0.13	0.49	0.59	0.63	0.78	0.84	0.89	0.94	0.97	1.00	1.03	1.07	1.09	1.12
EDB	0.14	0.53	0.64	0.73	0.86	0.93	0.98	1.05	1.06	1.09	1.14	1.19	1.26	1.30
1122TCA	0.13	0.42	0.55	0.62	0.68	0.72	0.75	0.77	0.78	0.82	0.84	0.90	0.92	0.96
NAPH	0.12	0.43	0.52	0.60	0.71	0.77	0.80	0.85	0.87	0.90	0.92	0.97	1.00	1.04

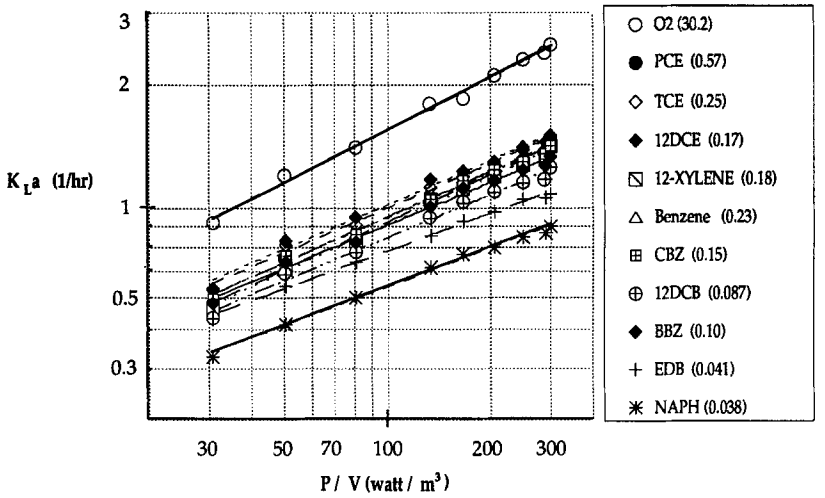

FIG. 5. Dependence of Mass-Transfer Coefficient on Specific Power Input

TABLE 3. Ratios of Gas-Phase to Liquid-Phase Mass-Transfer Coefficient

Rotational speed (RPM) (1)	P/V (W/m³) (2)	R (3)	k_Ga/k_La (4)	k_Ga (m/h) (5)
200	30.8	5.16E + 04	110.0	117.0
235	50.2	6.08E + 04	101.6	121.9
275	80.7	7.14E + 04	88.6	137.0
325	133.7	8.45E + 04	70.8	126.4
350	137.6	9.11E + 04	69.2	136.5
375	206.0	9.77E + 04	62.3	135.2
400	250.4	1.04E + 05	54.8	125.4
420	290.1	1.10E + 05	50.8	116.8
450	357.3	1.17E + 05	46.7	135.0
475	420.7	1.24E + 05	39.2	119.0
500	492.0	1.31E + 05	38.5	133.7

for the accuracy of the K_La-value. Eq. (20) can be transformed from logarithmic to the following exponential form:

$$C_L = C_{Lo} \exp[K_La(t - t_o)] \quad \ldots\ldots\ldots\ldots\ldots\ldots\ldots\ldots\ldots\ldots\ldots\ldots\ldots\ldots (21)$$

Using a two-parameter nonlinear regression, the concentration change over time can be used to determine the mass-transfer coefficient (K_La) and initial concentration (C_{Lo}) directly. This technique should provide greater precision since the entire data set is used to estimate C_{Lo}, as opposed to a single data point.

Table 2 shows the mass-transfer coefficients of 20 VOCs and oxygen for various impeller speeds (150–500 RPM). The specific power input (W/m³) is also shown. Fig. 5 shows the dependency of the mass-transfer coefficients (K_La) on specific power input (only 10 compounds are plotted for clarity).

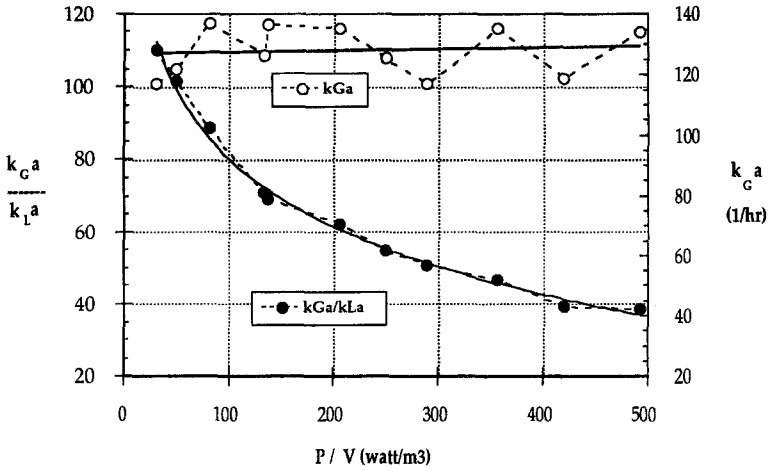

FIG. 6. Relationship of k_Ga and k_Ga/k_La to Specific Power Input (P/V)

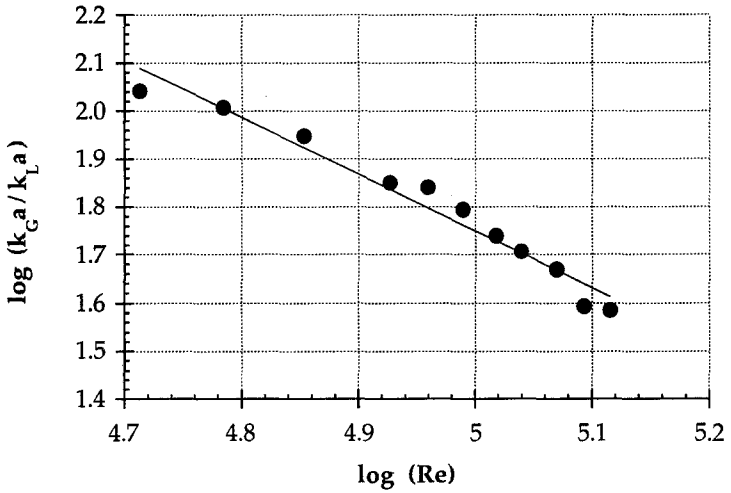

FIG. 7. Log(k_Ga/k_La) versus log(R)

The mass-transfer coefficients (K_La) increase with increasing power input and increasing H_c.

The ratios of oxygen gas-phase to liquid-phase mass-transfer coefficients (k_Ga/k_La) over the range of hydrodynamic conditions used here are listed in Table 3 and plotted in Fig. 6. The ratio was between 38 and 110 for experiments performed in the specific input range of 30–500 W/m^3. The estimated value of k_Ga/k_La in our experiments using the procedure in (16) was smaller than the widely assumed range of 50–300 (average ratio of k_Ga/k_La = 150) (Mackay and Leionoen 1975; Mackay et al. 1979). However, this range was higher than the 20–60 range reported in Munz's work (1984). Using a stirred-tank reactor with a turbine aerator in a closed system over a very wide range of power input (30–3,000 W/m^3) Libra (1991) found the

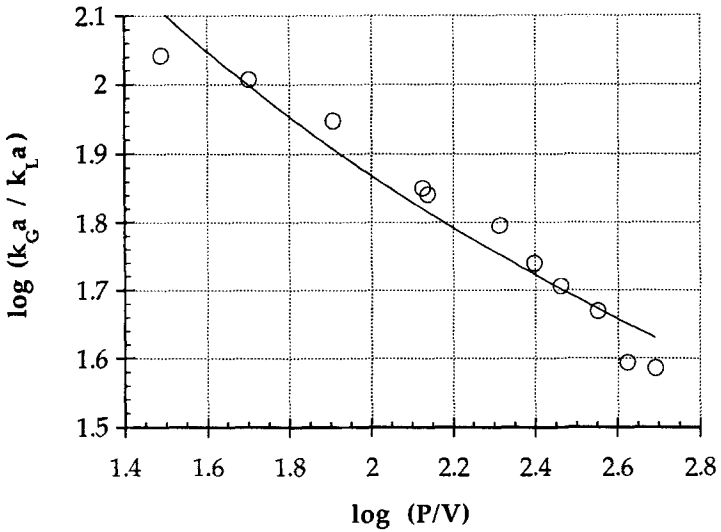

FIG. 8. Log($k_G a/k_L a$) versus log(P/V)

TABLE 4. Summary of Values of Ψ and Ψ_M

VOC (1)	Ψ (2)	S19 Ψ_M (3)	S26 Ψ_M (4)	S17 Ψ_M (5)	S22 Ψ_M (6)	S29 Ψ_M (7)	S27 Ψ_M (8)	S23 Ψ_M (9)	S32 Ψ_M (10)	S25 Ψ_M (11)
[RPM]	—	200	235	275	325	350	375	400	420	425
[$k_G a/k_L a$]	—	110.0	101.0	88.6	70.8	69.2	62.4	54.8	50.8	48.0
O_2	—	—	—	—	—	—	—	—	—	—
111TCA	0.65	0.64	0.64	0.64	0.64	0.64	0.63	0.63	0.63	0.63
PCE	0.65	0.64	0.64	0.64	0.63	0.63	0.63	0.63	0.63	0.63
CT	0.66	0.66	0.66	0.66	0.65	0.65	0.65	0.65	0.65	0.65
TCE	0.68	0.65	0.65	0.65	0.64	0.64	0.64	0.63	0.63	0.62
EBZ	0.60	0.58	0.58	0.57	0.57	0.57	0.56	0.56	0.55	0.55
12DCE	0.70	0.66	0.66	0.65	0.64	0.64	0.63	0.62	0.62	0.61
MXY	0.60	0.57	0.57	0.57	0.56	0.56	0.56	0.55	0.55	0.55
OXY	0.60	0.57	0.56	0.56	0.55	0.55	0.54	0.53	0.53	0.53
TLN	0.63	0.61	0.60	0.60	0.59	0.59	0.59	0.58	0.58	0.57
BZ	0.67	0.64	0.64	0.64	0.63	0.63	0.62	0.62	0.61	0.61
CLF	0.69	0.65	0.64	0.64	0.63	0.62	0.62	0.61	0.60	0.60
CBZ	0.64	0.59	0.59	0.58	0.57	0.57	0.56	0.56	0.55	0.55
13DCB	0.61	0.56	0.56	0.55	0.54	0.54	0.53	0.52	0.52	0.51
12DCB	0.61	0.54	0.53	0.52	0.51	0.50	0.50	0.48	0.48	0.47
14DCB	0.60	0.55	0.54	0.54	0.52	0.52	0.51	0.50	0.50	0.49
BBZ	0.63	0.56	0.56	0.55	0.53	0.53	0.52	0.51	0.50	0.50
BF	0.66	0.46	0.44	0.42	0.39	0.39	0.37	0.35	0.33	0.32
EDB	0.68	0.55	0.54	0.52	0.49	0.49	0.47	0.46	0.44	0.43
1122TCA	0.62	0.45	0.44	0.42	0.39	0.38	0.37	0.35	0.34	0.33
NAPH	0.58	0.45	0.45	0.43	0.40	0.40	0.39	0.37	0.36	0.35

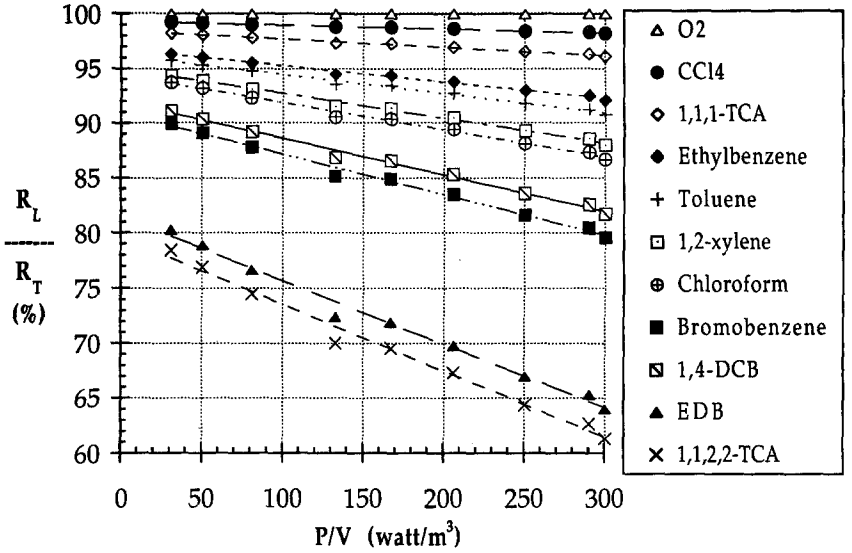

FIG. 9. Effect of Power Input on Liquid-Phase Resistance

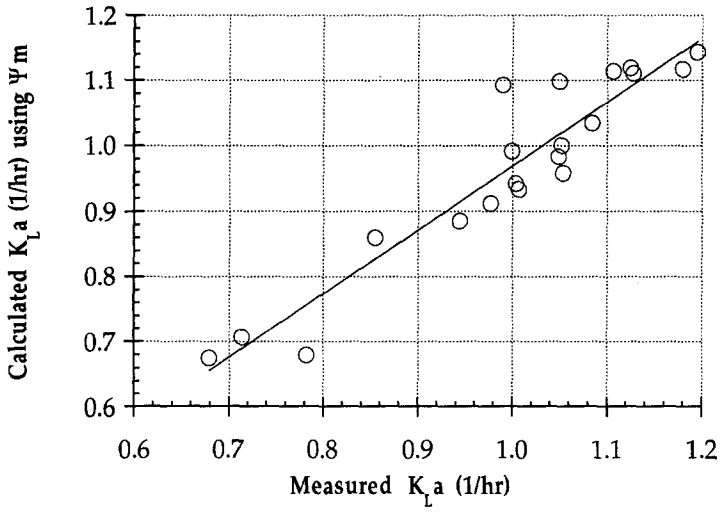

FIG. 10. Calculated and Measured Mass-Transfer Coefficient of 20 VOCs (325 RPM)

$k_G a/k_L a$ ratio to be as low as 0.1. These new results along with previous work suggest that the ratio is highly dependent upon experimental conditions. The ratio is not fixed. Fig. 6 also shows the relatively constant gas-phase mass-transfer coefficient ($k_G a$) because experiments performed with constant windspeeds of 1.8–2.4 (m/s) above the water surface. The average gas-phase mass-transfer coefficient ($k_G a$) obtained in this work is 126 ± 7 (1/h).

TABLE 5. Summary of Estimated and Measured Mass-Transfer Coefficients of 20 VOCs

VOC (1)	Overall ARE[a] (%) (2)	Test S19; 200 RPM			Test S26; 235 RPM			Test S17; 275 RPM			Test S22; 325 RPM			Test S29; 350 RPM		
		EST[b] (3)	PDT[c] (4)	ARE[a] (%) (5)	EST[b] (6)	PDT[c] (7)	ARE[a] (%) (8)	EST[b] (9)	PDT[c] (10)	ARE[a] (%) (11)	EST[b] (12)	PDT[c] (13)	ARE[a] (%) (14)	EST[b] (15)	PDT[c] (16)	ARE[a] (%) (17)
$[k_G a/k_L a]$	—	—	110.0	—	—	101.0	—	—	88.6	—	—	70.8	—	—	69.2	—
O_2	—	0.96	—	—	1.25	—	—	1.35	—	—	1.75	—	—	1.9	—	—
111TCA	5.4	0.58	0.62	−6.8	0.67	0.80	−19.9	0.87	0.86	0.9	1.11	1.11	−0.7	1.11	1.21	−8.9
PCE	4.8	0.56	0.61	−9.1	0.75	0.80	−6.5	0.83	0.86	−3.8	1.13	1.11	1.6	1.13	1.20	−7.0
CC14	5.8	0.64	0.63	1.0	0.78	0.82	−5.1	0.94	0.88	5.5	1.20	1.14	4.4	1.28	1.24	3.1
TCE	1.5	0.63	0.63	0.7	0.81	0.81	0.0	0.91	0.87	3.9	1.13	1.12	0.5	1.19	1.21	−1.7
EBZ	4.4	0.58	0.55	3.6	0.75	0.72	3.4	0.83	0.77	6.3	1.00	0.99	0.9	1.07	1.07	−0.9
12DCE	3.4	0.63	0.63	−0.4	0.83	0.82	0.8	0.95	0.88	7.1	1.18	1.12	5.3	1.23	1.21	1.6
MXY	6.9	0.57	0.55	3.9	0.65	0.72	−10.1	0.85	0.77	9.6	1.05	0.98	6.3	1.10	1.07	2.6
OXY	7.8	0.57	0.54	4.4	0.71	0.70	1.1	0.82	0.75	7.7	1.05	0.96	9.1	1.12	1.04	7.2
TLN	5.3	0.60	0.58	3.7	0.77	0.75	2.4	0.87	0.81	6.9	1.08	1.03	4.6	1.19	1.12	5.6
BZ	2.8	0.61	0.62	−2.0	0.75	0.80	−7.4	0.86	0.86	0.6	1.05	1.10	−4.5	1.17	1.19	−1.4
CLF	8.9	0.55	0.62	−12.6	0.71	0.80	−13.3	0.81	0.86	−5.8	0.99	1.09	−10.4	1.05	1.18	−12.8
CBZ	6.4	0.59	0.57	4.1	0.76	0.74	3.5	0.76	0.79	−3.1	1.05	1.00	4.9	1.17	1.08	7.4
13DCB	5.0	0.54	0.54	0.5	0.71	0.70	1.6	0.71	0.74	−5.0	1.00	0.94	6.2	1.06	1.02	3.8
12DCB	6.9	0.53	0.52	3.3	0.69	0.67	3.4	0.69	0.71	−2.5	0.94	0.89	6.2	1.03	0.96	7.3
14DCB	6.9	0.55	0.52	4.0	0.72	0.68	6.0	0.72	0.72	−0.2	0.98	0.91	6.7	1.08	0.99	8.7
BBZ	8.2	0.58	0.54	7.1	0.73	0.70	4.8	0.73	0.74	−1.2	1.01	0.93	7.4	1.12	1.01	9.9
BF	14.1	0.49	0.44	10.0	0.59	0.55	5.5	0.59	0.57	2.4	0.78	0.68	13.1	0.84	0.73	13.0
EDB	3.9	0.53	0.52	1.9	0.64	0.67	−3.9	0.64	0.70	−9.0	0.86	0.86	−0.5	0.93	0.93	0.1
1122TCA	1.8	0.42	0.43	−2.2	0.55	0.54	0.4	0.55	0.56	−3.2	0.68	0.67	0.7	0.72	0.73	−0.4
NAPH	4.8	0.43	0.44	−1.7	0.518	0.556	−7.3	0.52	0.58	−12.2	0.71	0.71	1.0	0.77	0.76	1.2
[Mean Error (%)]	5.8	—	—	[0.7]	—	—	[−2.0]	—	—	[0.2]	—	—	[3.1]	—	—	1.9
[Absolute mean value (%)]	—	—	—	[4.2]	—	—	[5.3]	—	—	[4.9]	—	—	[4.8]	—	—	5.2

[a]Absolute relative error (%) = (ESt* − PDT*)/EST* × 100%.
[b]Estimated $K_L a$.
[c]Predicted $K_L a$.

TABLE 6. Summary of Estimated and Measured Mass-Transfer Coefficients of 20 VOCs

VOC (1)	Test S27; 375 RPM			Test S23; 400 RPM			Test S32; 420 RPM			Test S25; 425 RPM		
	EST[a] (2)	PDT[b] (3)	ARE[c] (4)	EST[a] (5)	PDT[b] (6)	ARE[c] (7)	EST[a] (8)	PDT[b] (9)	ARE[c] (10)	EST[a] (11)	PDT[b] (12)	ARE[c] (13)
$[k_G a/k_L a]$	—	62.4	—	—	54.8	—	—	50.8	—	—	48	—
O_2	2	—	—	2.15	—	—	2.30	—	—	2.35	—	—
111TCA	1.25	1.27	−1.7	1.33	1.36	−2.1	1.38	1.45	−5.0	1.44	1.48	−2.3
PCE	1.21	1.26	−4.4	1.31	1.35	−3.6	1.37	1.44	−5.6	1.45	1.47	−1.8
CC14	1.41	1.30	7.4	1.54	1.40	9.2	1.63	1.49	8.3	1.67	1.53	8.5
TCE	1.28	1.27	0.9	1.39	1.35	2.9	1.45	1.44	0.5	1.51	1.47	2.8
EBZ	1.16	1.12	3.3	1.29	1.20	7.1	1.36	1.27	6.3	1.41	1.30	7.9
12DCE	1.30	1.26	3.0	1.41	1.34	5.5	1.46	1.42	2.7	1.49	1.44	3.7
MXY	1.19	1.11	6.6	1.28	1.19	7.5	1.35	1.26	6.7	1.41	1.28	9.0
OXY	1.20	1.08	9.8	1.28	1.15	10.2	1.33	1.22	8.0	1.42	1.24	12.8
TLN	1.26	1.17	7.2	1.33	1.25	6.3	1.37	1.33	3.5	1.46	1.35	7.7
BZ	1.26	1.24	1.5	1.33	1.32	0.9	1.34	1.41	−4.6	1.46	1.43	2.4
CLF	1.13	1.23	−9.6	1.25	1.31	−4.5	1.29	1.38	−7.8	1.36	1.40	−3.4
CBZ	1.25	1.13	9.5	1.30	1.19	8.2	1.36	1.26	7.2	1.42	1.28	10.0
13DCB	1.16	1.06	8.6	1.21	1.12	7.1	1.23	1.18	3.7	1.31	1.20	8.5
12DCB	1.09	0.99	9.5	1.15	1.04	10.0	1.18	1.09	7.3	1.26	1.10	12.3
14DCB	1.10	1.02	6.8	1.21	1.08	10.5	1.23	1.14	7.4	1.31	1.15	12.2
BBZ	1.17	1.04	10.7	1.24	1.10	11.5	1.27	1.16	8.9	1.34	1.17	12.6
BF	0.89	0.74	17.6	0.94	0.74	20.7	0.97	0.77	20.4	1.00	0.76	23.7
EDB	0.98	0.95	3.2	1.05	0.98	6.8	1.06	1.02	3.7	1.09	1.02	5.9
1122TCA	0.73	0.73	−0.3	0.77	0.75	2.5	0.78	0.77	0.9	0.82	0.77	5.9
NAPH	0.79	0.78	1.5	0.85	0.80	6.0	0.87	0.83	4.4	0.90	0.83	7.8
[Mean error (%)]	—	—	4.6	—	—	6.1	—	—	3.8	—	—	7.3
[Absolute mean value (%)]	—	—	6.2	—	—	7.2	—	—	6.1	—	—	8.1

[a]Estimated $K_L a$.
[b]Predicted $K_L a$.
[c]Absolute relative error (%) = (ESt* − PDT*)/EST* × 100%.

TABLE 7. Correlation between Calculated and Measured Mass-Transfer Coefficients

Rotational speed (RPM) (1)	P/V (W/m^3) (2)	a (3)	b (4)	R (5)
235	50.2	0.073	0.916	0.85
325	133.7	0.007	0.976	0.94
350	167.3	−0.020	1.000	0.91
375	206.0	−0.013	0.966	0.93
400	250.4	−0.088	1.013	0.95
420	290.1	−0.082	1.028	0.94
425	300.7	−0.014	1.036	0.95

Note: Calculated value = a + b(measured value)

Correlation of Mass Transfer Coefficients to Power Input

Munz and Roberts (1984) correlated the ratio of k_Ga/k_La to Reynolds number (R) as

$$\log\left(\frac{k_Ga}{k_La}\right) = -1.23\log(\mathrm{R}) + 7.06 \quad \ldots\ldots (22)$$

The correlation of this study shown in Fig. 7 is given as

$$\log\left(\frac{k_Ga}{k_La}\right) = -1.18\log(\mathrm{R}) + 7.66 \quad \ldots\ldots (23)$$

Comparing (22) and (23), the correlation observed in this study is very close to that of Munz and Roberts (1984). Munz and Roberts conducted their experiments in a fume hood with linear air velocities on the order of 2 m/s in the vicinity of the surface aeration reactor, which is similar to our condition (1.8–2.4 m/s). Therefore, k_Ga should be similar.

Due to the relatively constant windspeed, the ratio of k_Ga/k_La depends on the hydrodynamic condition of liquid phase. Both R and P/V are indicators of turbulence, but for high turbulence, R is independent of oxygen transfer or power input. Therefore, specific power input (P/V) is a better parameter for correlation and scale-up. The correlation of the ratio of k_Ga/k_La to P/V (W/m^3) is shown in Fig. 8. The correlation takes the form

$$\log\left(\frac{k_Ga}{k_La}\right) = -1.85\log\left(\frac{P}{V}\right) + 2.43 \quad \ldots\ldots (24)$$

A summary of Ψ and Ψ_M-values at each impeller speed (235–425 RPM) is given in Table 4. Since $\Psi_M = \Psi(R_L/R_T)$, the difference between Ψ and Ψ_M is a comparison of the significance of R_L/R_T. The R_L/R_T of 10 selected VOCs versus the specific power input is plotted in Fig. 9. For a given P/V, R_L/R_T decreases with decreasing H_c. For a given H_c, R_L/R_T is inversely proportional to P/V. The gas-phase resistance has very little effect on highly volatile compounds, such as oxygen, CCl_4, 1,1,1-TCA, and PCE. The gas-phase resistance has a significant effect on the compounds with H_c below 0.2, especially for low-volatility compounds, such as 1,4-DCB, 1,2-DCB,

EDB, bromoform, 1,1,2,2-TCA, and naphthalene. The impact of gas-phase resistance increases with increasing P/V.

Fig. 10 shows an example result for measured and estimated K_La at 325 RPM (134 W/m^3). Tables 5 and 6 show the estimated and measured K_La's for all impeller speeds from 235–425 RPM (31–300 W/m^3). Good agreement between observation and theory was obtained. The regression slopes for each power input are all very close to 1.0 (see Tables 5 and 6), but the intercepts decrease slightly with increasing power input, giving a consistent overestimation of $K_La_{O_2}$ at higher power inputs. The overestimation of $K_La_{O_2}$ may arise from entrainment of air bubbles, which increases the oxygen transfer. However, the increase of K_La_{VOC} is not proportional to the increase of $K_La_{O_2}$, because of the saturation of VOCs in the air bubbles. The average discrepancy between measured and estimated values of K_La of 20 VOCs for nine sets of experiments was 5.8% (Table 5). These errors may arise from the measurement of $K_La_{O_2}$ or K_La_{VOC} or the estimation of liquid diffusivity (Table 7). The estimation of liquid diffusivity has an error of 10–15% (Reid et al. 1986).

CONCLUSIONS

This research extends the current concepts for estimating VOC transfer to include the effects of gas-phase resistance.

A new concept, Ψ_M, using ratio of the diffusivity of the VOC to oxygen corrected with liquid-phase resistance is introduced. Excellent agreement between theory and observation for 20 VOCs over a range of hydrodynamic conditions and Henry's coefficients (H_c) was obtained.

For a given specific power input, the liquid-phase resistance increases with decreasing H_c. The gas-phase resistance has a very significant effect for compounds with $H_c < 0.2$ under the hydrodynamic conditions examined in this research. For a given compound, liquid-phase resistance significantly decreases with increasing specific power input.

The ratio of gas to liquid-phase transfer coefficients (k_Ga/k_La) depends upon the mixing conditions of the liquid and gas phases, which are a function of the specific experimental or process conditions. Experiments performed with constant windspeed of 1.8–2.4 m/s resulted in a relatively constant gas-phase mass-transfer coefficient (k_Ga) of 126 (1/h). The k_Ga/k_La ratio decreases with increasing specific power input, because the gas-phase transfer coefficient is unaffected by power change in the liquid phase.

Using the Ψ concept without accounting for gas-phase resistance for semivolatile compounds significantly overestimates stripping loss.

ACKNOWLEDGMENT

This research was supported in part by the NSF funded Engineering Research Center on Hazardous Substance Control and a fellowship from BP-America. We acknowledge Dr. Jack Lee for his help with the use of the SAS model in analyzing the data, and give special thanks to Eddy C. T. Tzeng for his assistance in GC analysis. We thank Dr. Judy A. Libra for her contributions to this research.

APPENDIX I. REFERENCES

Standard methods for the examination of water and wastewater. (1985). 16th Ed., American Public Health Association (APHA), Washington, D.C.

ASCE Oxygen Transfer Standards Committee. (1984). *A standard for the measurement of oxygen transfer in clean water.* ASCE, New York, N.Y.
Baillod, C. R., Crittenden, J. C., Mihelcic, J. R., Rogers, T. N., and Grady, L. (1990). "Transport and fate of toxics in wastewater treatment facilities." *Res. Found. Proj. 90-1*, Water Environment Federation (WEF), Alexandria, Va.
Danckwerts, P. V. (1951). "Significance of liquid-film coefficient in gas absorption." *Ind. Engrg. Chem.*, 43(6), 1460–1467.
Dobbins, W. E. (1964). "Mechanism of gas absorption by turbulent liquids." *Proc., Int. Conf. Water Pollution Res.*, Pergamon Press, London, England, 61–76.
Eckenfelder, W. W., and Ford, D. L. (1967). "Engineering aspects of surface aeration design." *Proc., 22nd Purdue Industrial Waste Conf.*, Purdue University, Lafayette, Ind., 279–291.
Goodgame, T. H., and Sherwood, T. K. (1954). "The additivity of resistances between phases." *Chem. Engrg. Sci.*, 3(2), 37–42.
Gossett, J. M. (1987). "Measurement of Henry's law constants for C1 and C2 chlorinated hydrocarbons." *Envir. Sci. and Tech.*, 21(2), 202–208.
Higbie, R. (1935). "The rate of absorption of a pure gas into a still liquid during short periods of exposure." *Trans. AIChE*, 31, 365–388.
Hsieh, C.-C. (1991). "Estimating volatilization rates and gas/liquid mass transfer coefficients in aeration systems," PhD thesis, University of California, Los Angeles, Calif.
Kozinski, A. A., and King, C. J. (1966). "The influence of diffusivity on liquid phase mass transfer to the free surface in a stirred vessel." *AIChE J.*, 12, 109–116.
Lewis, W. K., and Whitman, W. G. (1924). "Principles of gas absorption." *Ind. Engrg. Chem.*, 16, 1215–1220.
Libra, J. A. (1991). "Volatilization of organic compounds in an aerated stirred tank reactor," PhD thesis, University of California, Los Angeles, Calif.
Mackay, D., and Leinonen, P. J. (1975). "Rate of evaporation of low-solubility contaminants from water bodies to atmosphere." *Envir. Sci. and Tech.*, 9(13), 1178–1180.
Mackay, D., Shiu, W. Y., and Sutherland, R. P. (1979). "Determination of air-water Henry's law constants for hydrophobic pollutants." *Envir. Sci. and Tech.*, 13(9), 333–337.
Mackay, D., and Shiu, W. Y. (1981). "A critical review of Henry's law coefficients for chemicals of environmental interest." *J. Phys. Chem. Ref. Data*, 10(4), 1175–1199.
Mackay, D., and Yeun, A. T. K. (1983). "Mass transfer coefficient correlations for volatilization of organic solutes from water." *Envir. Sci. and Tech.*, 17(4), 211–217.
Matter-Mueller, C., Gujer, W., and Giger, W. (1981). "Transfer of volatile substances from water to the atmosphere." *Water Res.*, 15, 1271–1279.
Munz, C., and Roberts, P. V. (1984). "The ratio of gas phase to liquid phase mass transfer coefficients in gas-liquid contacting processes." *Gas transfer at water surfaces*, W. Brutsaert and G. H. Jirka, eds., D. Reidel Publishing Co., Hingham, Mass., 35–45.
Munz, C., and Roberts, P. V. (1986). "Effects of solute concentration and cosolvents on the aqueous activity coefficient of halogenated hydrocarbons." *Envir. Sci. and Tech.*, 20, 830–836.
Munz, C., and Roberts, P. V. (1987). "Air-water phase equilibria of volatile organic solutes." *J. AWWA*, 79(1), 62–69.
Paulson, W. C. (1979). "Review of test procedures." *Proc., Workshop Towards and Oxygen Transfer Standard; EPA-600/9-78-021*, W. C. Boyle, ed., Municipal Environmental Research Laboratory, U.S. Environmental Protection Agency, Cincinnati, Ohio, 41–49.
Perry, and Green. (1984). *Perry's chemical engineer's handbook*, 6th Ed., McGraw-Hill Book Co., Inc., New York, N.Y.
Reid, R. C., Prausnitz, J. M., and Sherwood, T. K. (1987). *The properties of gases and liquids*, 4th Ed., McGraw-Hill Book Co., Inc., New York, N.Y.
Roberts, P. V., and Dandliker, P. G. (1983). "Mass transfer of volatile organic

contaminants from aqueous solution to the atmosphere during surface aeration." *Envir. Sci. and Tech.*, 17(8), 484–489.
Roberts, P. V., Munz, C., and Dandliker, P. (1984). "Modeling volatile organic solute removal by surface and bubble aeration." *J. WPCF*, 56(2), 157–163.
SAS user's guide; statistical analysis system. (1982). SAS Institute Inc., Raleigh, N.C.
Nagata, S. (1975). *Mixing principles and applications.* John Wiley and Sons, New York, N.Y.
Smith, J. H., Bomberger, D. C., and Haynes, D. L. (1980). "Prediction of the volatilization rates of high-volatility chemicals from natural water bodies." *Envir. Sci. and Tech.*, 14(11), 1332–1337.
Treybal, R. E. (1968). *Mass transfer operations*, 2nd Ed., McGraw-Hill Book Co., Inc., New York, N.Y.
Verschueren, K. (1977). *Handbook of environmental data on organic chemicals.* Van Nostrand Reinhold Co., New York, N.Y.

APPENDIX II. NOTATION

The following symbols are used in this paper:

a = interfacial area;
C = concentration;
D_G = gas diffusivity;
D_L = liquid diffusivity;
H = Henry's coefficient;
H_c = dimensionless Henry's coefficient;
K = overall mass-transfer coefficient;
k = mass-transfer coefficient;
M = gram molecular weight;
m = exponent of gas diffusivity;
N = rotational speed;
n = exponent of liquid diffusivity;
P = power input;
p = vapor pressure;
R = film resistance;
S = solubility;
t = time;
V = volume;
Ψ = ratio of mass-transfer coefficients of VOC to oxygen; and
Ψ_M = modified Ψ.

Subscripts

G = denotes gas phase
L = denotes liquid phase
O_2 = denotes oxygen
o = denotes initial
T = denotes total; and
VOC = denotes volatile organic compound.

Superscript

* = denotes saturation.